

NASA/TM—1999-209044



Electrical Breakdown of Anodized Structures in a Low Earth Orbital Environment

J.T. Galofaro
Glenn Research Center, Cleveland, Ohio

C.V. Doreswamy
Tuskegee University, Tuskegee, Alabama

B.V. Vayner
Ohio Aerospace Institute, Cleveland, Ohio

D.B. Snyder and D.C. Ferguson
Glenn Research Center, Cleveland, Ohio

National Aeronautics and
Space Administration

Glenn Research Center

April 1999

This report is a formal draft or working paper, intended to solicit comments and ideas from a technical peer group.

This report contains preliminary findings, subject to revision as analysis proceeds.

Trade names or manufacturers' names are used in this report for identification only. This usage does not constitute an official endorsement, either expressed or implied, by the National Aeronautics and Space Administration.

Available from

NASA Center for Aerospace Information
7121 Standard Drive
Hanover, MD 21076
Price Code: A03

National Technical Information Service
5285 Port Royal Road
Springfield, VA 22100
Price Code: A03

ELECTRICAL BREAKDOWN OF ANODIZED STRUCTURES IN A LOW EARTH ORBITAL ENVIRONMENT

J.T. Galofaro^{*}
National Aeronautics and Space Administration
Glenn Research Center
Cleveland, Ohio 44135

C.V. Doreswamy[†]
Tuskegee University
Tuskegee, Alabama 36088

B.V. Vayner,[‡] D.B. Snyder,[§] and D.C. Ferguson[¶]
National Aeronautics and Space Administration
Glenn Research Center
Cleveland, Ohio 44135

SUMMARY

A comprehensive set of investigations involving arcing on a negatively biased anodized aluminum plate immersed in a low density argon plasma at low pressures ($P_0 \approx 7.5 \times 10^{-5}$ torr) have been performed. These arcing experiments were designed to simulate electrical breakdown of anodized coatings in a Low Earth Orbital (LEO) environment. When electrical breakdown of an anodized layer occurs, an arc strikes, and there is a sudden flux of electrons accelerated into the ambient plasma. This event is directly followed by ejection of a quasi-neutral plasma cloud consisting of ejected material blown out of the anodized layer. Statistical analysis of plasma cloud expansion velocities have yielded a mean propagation velocity, $v = (19.4 \pm 3.5)$ km/s. As the plasma cloud expands into the ambient plasma, energy in the form of electrical noise is generated. The radiated electromagnetic noise is detected by means of an insulated antenna immersed in the ambient plasma. The purpose of the investigations is (1) to observe and record the electromagnetic radiation spectrum resulting from the arcing process. (2) Make estimates of the travel time of the quasi-neutral plasma cloud based on fluctuations to several Langmuir probes mounted in the ambient plasma. (3) To study induced arcing between two anodized aluminum structures in close proximity.

NOMENCLATURE

- C capacitance, F
- D plate separation, m
- E electrical field strength, V/m
- f frequency, Hz
- L antenna length, m
- N_e electron number density, m^{-3}
- OD outer diameter, m

^{*}Physicist, (Dept.), E-mail: joel.t.galofaro@grc.nasa.gov. Member AIAA.

[†]Professor, Tuskegee University, Tuskegee, AL 36088.

[‡]Senior Research Associate, (Dept.), Ohio Aerospace Institute. Member AIAA.

[§]Physicist, (Dept.), Member AIAA.

[¶]Senior Scientist, (Dept.), Member AIAA.

P_0	neutral gas pressure, torr
R	resistance, Ω
r	probe and plate distance, m
T_e	electron temperature, eV
V	bias potential, V
v	average velocity, m/s
W	width, m
$\Delta\tau$	propagation time, s
Δx	thickness of anodized layer, m
v	mean velocity, m/s
ϕ_b	plate bias potential, V

INTRODUCTION

The trend for modern day satellite payloads is for more robust, higher voltage power systems. Where older payloads typically operated at less than 80 V, newer payloads currently operate at just under 200 V. The higher voltages have placed a heavier demand on spacecraft power systems, and the trend is ever increasing as payloads become more complex. Historically spacecraft have incorporated a negative grounding scheme into their structures in order to provide a single point ground connection for electrical components. The typical way of providing a negative ground is to tie the negative end of the solar array directly to the structure of the spacecraft. The negative grounding scheme has led to other potentially hazardous problems involving arcing. Furthermore it has been found that both the solar arrays and the structure are vulnerable to arcing. These arcing concerns has led to other matters involving electromagnetic interference (EMI) with scientific payloads which also need to be addressed. For example, in order to provide the required power for the International Space Station (ISS), the operating voltage was set to 160 V (ref. 1). This 160 V, coupled with the negative grounding scheme, has unfortunately placed the ISS in a region where there are significant physical interactions with the LEO plasma (refs. 1 to 3). The series of experiments will focus on one such interaction, the electrical breakdown of anodized coatings (i.e., structures) in a Low Earth Orbit (LEO) environment.

Insulating paints are often used to passively regulate the surface temperature of spacecraft structures in LEO (refs. 4 and 5). More recently several types of anodized coatings have been developed for use on the ISS. A chromic acid anodized coating, produced by the type I or type IB process, with a thickness between 1.3 to 5.1 μm was finally decided upon for the ISS (refs. 1 and 6). The thickness of these coatings has been manufactured to supply the needed thermal properties for temperature stabilization of external surfaces, as well as providing protection against atomic oxygen degradation.

It has been shown that the 160 V solar array of the ISS will cause the structure to charge between -120 and -140 V relative to local plasma potential (refs. 1 and 2). Unfortunately the thickness of the anodized surfaces specified for the ISS do not have sufficient dielectric strength to be able to stand off the -120 to -140 V they may acquire (refs. 1, 7 and 8). In order to fix its problems the ISS has baselined the use of a plasma contactor. Depending on the design voltage specified for new high voltage power systems, future spacecraft may need to use thicker anodized coatings to protect against such interactions.

EXPERIMENTAL TEST APPARATUS

Ground tests were performed at NASA's Glenn Research Center (GRC) Plasma Interaction Facility (PIF). All the experiments were conducted in the 1.8-m diameter by 3.0-m high vertical vacuum chamber. Two Penning discharge sources, equipped with a 0.25-mm diameter tungsten filament, were used to ionize argon gas molecules and provide plasma for the experiments. Neutral gas pressures were carefully monitored

and maintained at $P_0 = 7.5 \times 10^{-5}$ torr throughout the tests with the plasma sources operating. Plasma densities (N_e) ranged between 1.8 to 8.6×10^5 [electrons/cm³] and electron temperatures (T_e) were on the order of 1.2 to 1.3 eV.

For these experiments several type II, class 1, sulfuric acid anodized aluminum plates, with an alloy designation of 6061-T6 (having a specified minimum coating thickness of 2.5146 μm (ref. 1) and conforming to MIL-A-8625E, were procured. The T6 coating designation calls for tempering an aluminum alloy by heat treatment prior to anodizing a coating electrolytically in a sulfuric acid bath.

The anodized aluminum plates arrived as six precut 30.48 \times 30.48 cm plates and one large 60.96 \times 60.96 cm plate which were anodized on both sides. The center conductor of a shielded coaxial cable (RG-58/U, 50 Ω) was attached to each plate and terminated with a standard BNC connector on the other end. The anodized plates were prepared by covering the sides and back with a 0.05-mm kapton sheet. The plates were then cleaned with an isopropyl alcohol wash and allowed to air dry prior to mounting them in the tank. The BNC's were attached to an insulated electrical feedthrough rated at 1000 V breakdown potential.

Diagnostic equipment consisted of two spherical Langmuir probes (1.9-cm diameter) and two cylindrical wire probes (0.32-cm diameter \times 5.08-cm long). Two antennae were constructed, each with 0.32-cm diameter \times 56.56-cm long insulated whips, and identical 47 \times 47-cm hexagonal ground planes which were fashioned from 0.32-cm aluminum sheet metal. A very sensitive current probe amplifier and current probe were also used. Dual channel (300 and 330 MHz) digitizing oscilloscopes, each equipped with an IEEE-488 bus, were also used to capture and store measurements in a very short time interval.

The mounting positions of the probes inside the vacuum chamber are shown in figure 1. All probes, with the exception of antenna B, are mounted at a height of 59.69 cm high off the subfloor of the vacuum tank. Table I identifies the measured distance of each probe with respect to the center of the anodized plate.

Figure 2 shows a pictorial diagram of experimental apparatus used in obtaining the electromagnetic frequency spectrum, and for the plasma cloud propagation tests. The diagram shows an anodized aluminum plate biased negative of tank ground by a high voltage DC power supply. The DC power supply charges a 0.47 μF capacitor, which is mounted in parallel with the DC power supply and the anodized plate. The value of the capacitor is used to represent the capacitance of a typical satellite in space. Note that when electrical breakdown of the anodized coating occurs, an arc strikes, and the arc return path is through the plasma and back to tank ground. In order for charge to be conserved, the same current must flow from the negative terminal of the capacitor and back to the anodized plate. A current probe is placed between the negative capacitor terminal and the plate in order to detect an arc. When the current probe detects an arc, the signal is amplified, and sent to channel 2 which has been set to trigger at a given current level. Channel 2 of the first scope then simultaneously triggers channel 1 and both channels on the second scope via an external trigger. In this way 4 channels of information are gathered at once.

The diagram in figure 3 depicts the experimental setup used for the induced arcing experiments. For these experiments identical pairs of anodized aluminum plates were mounted in parallel (with the exposed anodized surfaces of the plates facing one another) and floated in the ambient plasma. Note that there are two arcing circuits shown and each plate is independently biased negative relative to tank ground through a separate DC power supply. An initial arc on plate A simultaneously triggers both channels on the LeCroy 4950A scope.

EXPERIMENTAL RESULTS

Measurements of the electromagnetic radiation spectrum resulting from the arcing process were obtained. Being only interested in obtaining electromagnetic interference (EMI) measurements generated by the arcing process, the antenna whips needed to be insulated, thereby passing all radiated emissions and effectively blocking the conducted emissions caused by the expansion of the plasma cloud into the ambient plasma. Both antennae were cut to a resonant frequency of 500 MHz in order to give a broad band behavior at the measured frequencies. The antenna leads were cut according to the equation: $L = (299.8)(0.95)/f$, where L is the length in meters and f is the frequency in megahertz. All data were obtained in digital form with a sampling interval of 2.5-ns. This sampling rate yields a maximum bandwidth of 200 MHz for the tests. A Fast Fourier Transform was applied to the data in order to map signals from the time domain to a frequency domain for comparison against the SSF specification for electromagnetic interference (EMI).

Two perpendicular antennae were used to find the direction and strength of the electromagnetic field. Thus antennae A and B were mounted in orthogonal directions, to measure the components (signal strength versus time) of arc induced electromagnetic radiation generated in each of the respective directions. Which explains why there are two sets of results shown for each antenna.

Figures 4(a) and (b) show typical electromagnetic signatures picked up by the horizontally mounted insulated antenna, as well as the resultant electromagnetic frequency spectrum obtained by the horizontal antenna.

Similar data were recorded for the vertical antenna (see figs. 5(a) and (b)). Note that the magnitude of the frequency plots is in relative units. The E-field strength was estimated as 0.5 [V/m/MHz]. The EMI standards for the ISS, are given in units of dB [μ V/m/MHz] (refs. 9 and 11).

It was found that the EMI levels for the horizontal and vertical antennae exceed the EMI standards set fourth for Space Shuttle (refs. 9). Figures 6(a) and (b) show the EMI level of arcs on an anodized aluminum plate converted to units of decibels. Figure 6(a) demonstrates quantitatively the safe EMI level specified for the Space Shuttle is exceeded. Figure 6(b) shows similar data for payloads in the Shuttle payload bay, which are held to a more rigorous EMI standard. Note that data plotted in figures 6(a) and (b) are the result of 34 separate ground based antennae measurements of EMI levels due to arcs on anodized aluminum plates. The next set of measurements involved determining the travel time of the expanding plasma cloud caused by the arcing process. Noninsulated probes were used in order to pass the conducted emissions. As previously discussed when an arc strikes, a quasi-neutral cloud of material is ejected into the ambient plasma. Experiments have shown that a single arc on an anodized aluminum plate may generate as many as 10^{15} atoms of aluminum into the surrounding plasma (ref. 10).

It is possible to measure the overall time response of the probe to the arcing process and hence make travel time estimates based on the difference in time Δt between when an arc event initially occurs and when the wire probe finishes sensing the perturbations causing the arc. (See fig. 7.) The upper trace displays the initial arc event, which is initially triggered by an arc on plate Ny1. The lower trace, which was simultaneously triggered, displays what is sensed by the wire probe. It is important to note that the plasma cloud first begins to sense the wire probe, approximately 10 μ s later than the initial arc trigger at point (A). The plasma cloud oscillations are fully developed by the time point (P) is reached. Point (B) designates the time just before the rise of the small pulse at point (E) is sensed. The small oscillation at Point (E) is due to electrical field fluctuations generated by breakdown of the anodized coating. This pulse at point (E) marks the end of the arcing process. Hence, the travel time is equal to difference in time Δt between points (A) and (B). Table II tabulates the plasma cloud travel times for various probes. Because the distance from the plate to each probe are known (see table I) the average velocity of expanding plasma cloud can be calculated. These values are shown in table II. A statistical analysis of the plasma cloud expansion velocities shown in table II yield a mean propagation velocity, $v = (19.4 \pm 3.5)$ km/s. Note that one could have judiciously chosen the peak values at points (P) and (E) for the travel time estimates. In this case the travel time estimate would have been shorter.

The final set of experiments involved induced arcing between two parallel plates of anodized aluminum in close proximity. The purpose of these experiments was to verify that an initiating arc on plate, A, would cause an arc to be triggered on plate B. Plate A was negatively biased at a potential above the arcing threshold. Plate B was set to a less negative potential, just under the arcing threshold. It was felt an arc triggered on plate A, could temporally pull plate B more negative than the bias potential set on plate B. The net voltage drop could cause electrical breakdown of the anodized coating on plate B.

For these tests the sulfuric acid anodized coatings (Type II, MIL-A-8265E) were abandoned for some of the chromic acid anodized coatings (Type I, MIL-A-8265E) used in the previous summer's experiments. The chromic acid anodized plates arced at nearly half the voltage (-200 V) that of the sulfuric acid anodized plates. (The sulfuric acid anodized samples were found to arc at approximately -400 V.) Since the chromic acid anodized plates were manufactured to the same coating thickness, $\Delta x = 2.5$ μ m, this equates to a 50 percent reduction in the E-field strength, or $E = 7.9 \times 10^7$ V/m, before arcing can occur in the chromic acid anodized coatings. As a result the chromic acid anodized coatings better represent the actual charging potentials that may be seen on ISS when no plasma contactor is present. Because only a small amount of the anodized material was available at the time of these tests, the samples were cut into smaller 18 \times 18-cm plates for these experiments. Sample pairs were mounted in the tank with a separation of 25 and 50 cm between each parallel plate pair. One parallel plate in each pair was biased at -250 V potential. The remaining plate in each pair biased at -300 V.

Figures 8(a) and (b) show the current registered by two independently biased parallel plates separated by 50 cm. Figures 9(a) and (b) demonstrate induced arcing between two independently biased parallel plates at a distance of 25 cm from one another. Note that the arc pulses are of comparable height here. The delay time could not be measured due to the time scale of the waveforms. What is certain is that the time delay is not due to influences caused by expansion of the plasma cloud, which is on the order of 20 to 40 μ s. Hence arcs on plate A and plate B appear to be simultaneously triggered. In figures 8 and 9 the initiating arc is believed to occur on plate A, since plate B is below the arcing threshold.

CONCLUSION

Much valuable information important to the ISS, spacecraft designers and the scientific community in general has been obtained as a result of these tests. With the current setup we have been able to successfully record the electromagnetic radiation spectrum resulting from the arcing process. It was found that the frequency spectrum peaks between 8 and 10 MHz and that the magnitude of interference exceeds the EMI the technical specifications set for Space Shuttle operation. Accurate estimates of the time of travel of the expanding plasma cloud resulting from the arcing process were also made. Measurements have ascertained the velocity of the expanding plasma cloud (19.4 ± 3.5) km/s is somewhat lower than earlier estimates of (25 to 30) km/s¹. These velocities are highly dependent on the points chosen for the travel time estimates. Finally, it has been demonstrated that induced arcing between two independently biased anodized plates is possible. Induced arcing could have serious consequences for high power instrument payloads operating in the Shuttle payload bay.

REFERENCES

1. Vaughn, J.A., Carruth Jr., M.R., Katz, I., Mandell, M.J., and Jongeward, G.A.: "Electrical Breakdown Currents on Large Spacecraft in Low Earth Orbit," *Journal of Spacecraft and Rockets*, Vol. 31, No. 1, 1994, pp. 54-59
2. Kennerude, K.L.: "High Voltage Array Experiments," NASA CR-121280, March 1994
3. McCoy, J.E., and Konradi, A.: "Sheath Effects Observed on a 100 Meter High Voltage Panel in Simulated Low Earth Orbit," *Proceedings of Spacecraft Charging Technology 1978*, NASA CP-2071, Oct.-Nov. 1978 pp. 201-210
4. Robinson, P., and Whittlesey, A.: "Electrostatic Charging Characteristics of Thermal Control Paints as a Function of Temperature," *Proceedings of Space Charging Technology 1980*, NASA CP-2182, Nov 12-14, 1980 pp. 309-319.
5. Leung, P.: "The Electrical Conductivity of ZOT After a Long Term Exposure to Thermal Vacuum Environment," *Proceedings of Spacecraft Charging Technology Conference 1989*, Oct-Nov 1989, pp. 166-173
6. Military Specification MIL-A-8625E: "Anodic Coatings for Aluminum and Aluminum Alloys," Navy-AS MFFP-0368, April 25, 1988, pp. 1-18
7. Carruth, M.R. Jr., Vaughn, J.A., and Gray, P.A.: "Experimental Studies of Spacecraft Arcing," AIAA Paper 92-0820 Jan. 1992
8. Carruth, M.R. Jr., Vaughn, J.A., Holt, J.M., Werp, R., and Sudduth, R.D.: "Plasma Effects on Passive Thermal Control Coatings of Space Station Freedom," AIAA Paper 92-1685, March 1992
9. Vayner, B.V., Doreswamy, C.V., Ferguson, D.C., Galofaro, J., and Snyder, D.B.: "Arcing on Aluminum Anodized Plates Immersed in Low-Density Plasmas," *Journal of Spacecraft and Rockets*, Vol. 35, No. 6, September-October 1998, pp. 805-811
10. B.V. Vayner, B.V., Ferguson, D.C., and Galofaro, J.: "The Spacecraft Surfaces Degradation and Contamination Caused by Arcing in Low Density Plasmas," XVIII ISDEIV Conference, Eindhoven, Netherlands, Aug 17-21, 1998 pp. 824-827
11. Vayner, B.V., Ferguson, D.C., and Snyder, D.B.: "Electromagnetic Radiation Generated by Arcing in Low Density Plasma," NASA TM-107217, July 1996.

TABLE I.—PROBE DIMENSIONS AND MOUNTING POSITIONS SPECIFIED FOR THE VERTICAL CHAMBER TESTS

[Note: All radii (r) measured from center of plate 1. D = plate separation distance. OD = outer diameter.]

Probe number	Probe type	Dimension	Distance
LP1	Wire probe 1	0.3175 cm OD × 5.08 cm L	r = 57.15 cm
LP2	Spherical probe 2	1.905 cm OD	r = 48.89 cm
LP3	Wire probe 2	0.3175 cm OD × 5.08 cm L	r = 77.47 cm
LP4	Spherical probe 1	1.905 cm OD	r = 78.74 cm
A&B	Antenna lead Hexagonal ground plane	0.3175 cm OD × 56.96 cm L 47 cm × 47 cm	r = 100 cm
Plate 1	Large anodized plate Parallel anodized plates	60.96 cm L × 60.96 cm W 18 cm L × 18 cm W	D = 25.50 cm

TABLE II.—TABULATED RESULTS FOR PLASMA CLOUD TRAVEL TIMES, VELOCITY AND FREQUENCY

Probe type	$\Delta t = (\tau - \tau_0)$	$v = (\Delta x / \Delta t)$	$f = 1 / \Delta t$
Wire probe 1	28.8 μ S	19.8 km/S	34.7 kHz
Wire probe 1	34.1 μ S	16.8 km/S	29.3 kHz
Wire probe 1	28.7 μ S	19.9 km/S	34.7 kHz
Wire probe 1	30.9 μ S	18.5 km/S	32.4 kHz
Wire probe 2	37.3 μ S	20.8 km/S	26.8 kHz
Wire probe 2	34.2 μ S	22.7 km/S	28.2 kHz
Wire probe 2	32.5 μ S	23.8 km/S	30.8 kHz
Wire probe 2	35.0 μ S	22.1 km/S	28.6 kHz
Sphere LP2	31.3 μ S	15.6 km/S	31.9 kHz
Sphere LP2	34.1 μ S	15.6 km/S	29.3 kHz
Sphere LP2	34.3 μ S	14.3 km/S	29.2 kHz
Sphere LP2	20.3 μ S	24.1 km/S	49.3 kHz

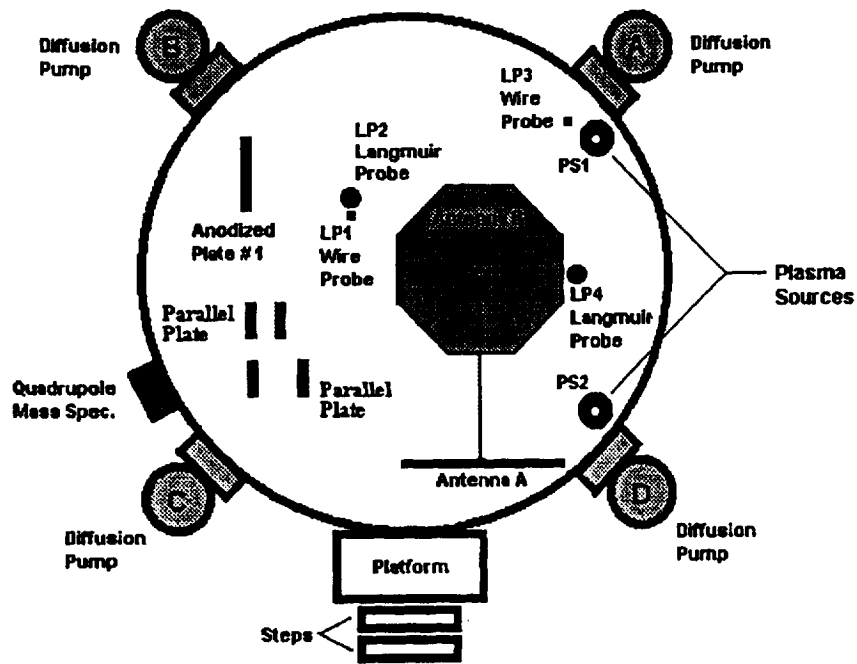


Figure 1.—Top down cutaway view of vertical Chamber,
(Dimensions: 1.8 μm diameter x 3.0 μm high)

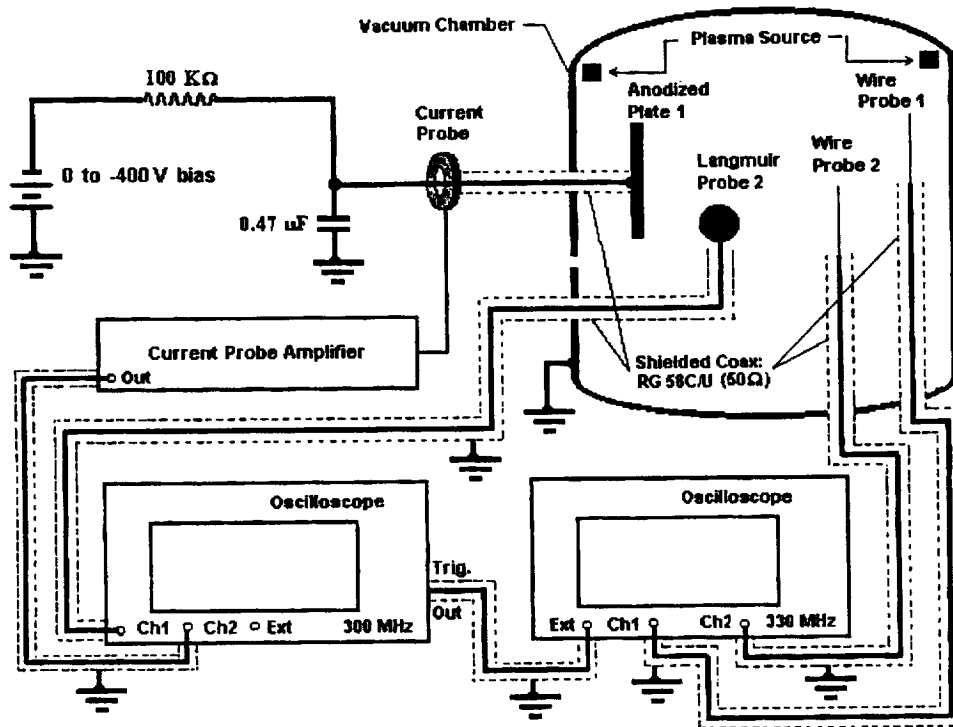


Figure 2.—Experimental apparatus for the electromagnetic frequency spectrum measurements and plasma cloud propagation experiments.

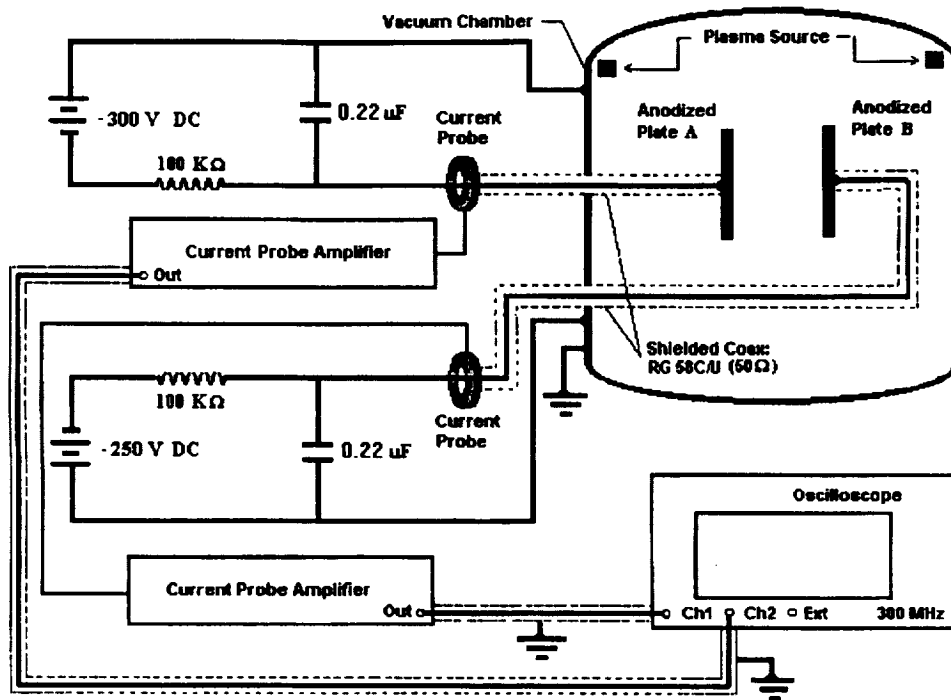


Figure 3.—Experimental apparatus for the induced arcing experiments.

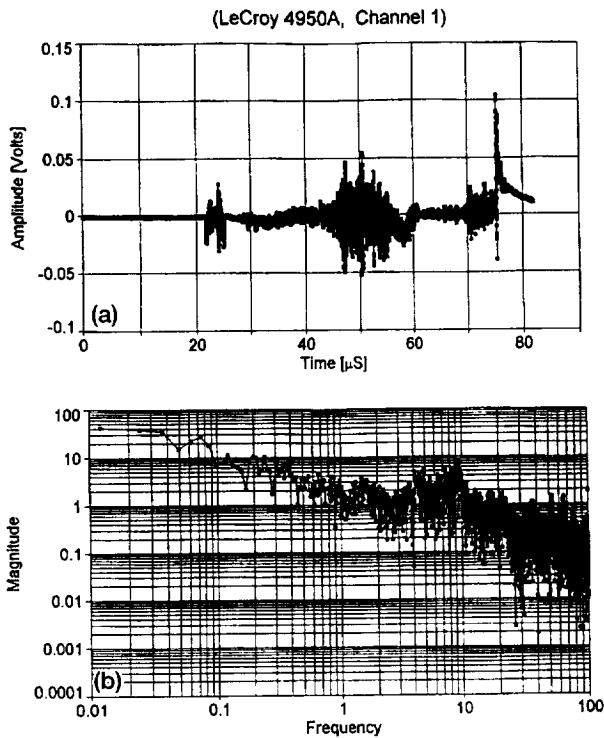


Figure 4.—(a) Electromagnetic signature resulting from arc. Signal trace shown was acquired from the horizontal antenna (Antenna A). (b) Resultant electromagnetic frequency spectrum for the horizontal antenna. Displayed waveform was obtained from the Fourier Transform of signal trace in figure (a) (note: frequency in MHz and vertical scale is given in relative units).

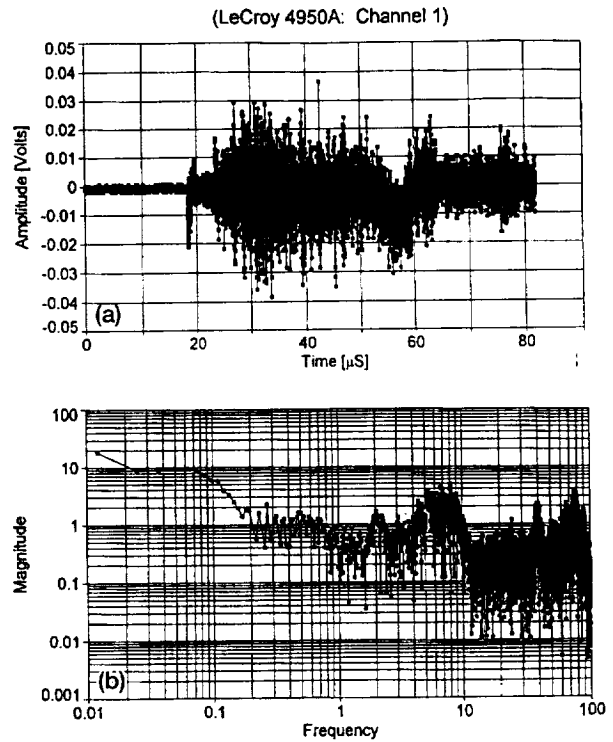


Figure 5.—(a) Electromagnetic signature resulting from arc. Signal trace shown was acquired from the vertical antenna (Antenna B). (b) Resultant electromagnetic frequency spectrum for the vertical antenna. Displayed waveform was obtained from the Fourier Transform of signal trace in figure (a) (note: frequency in MHz and vertical scale is given in relative units).

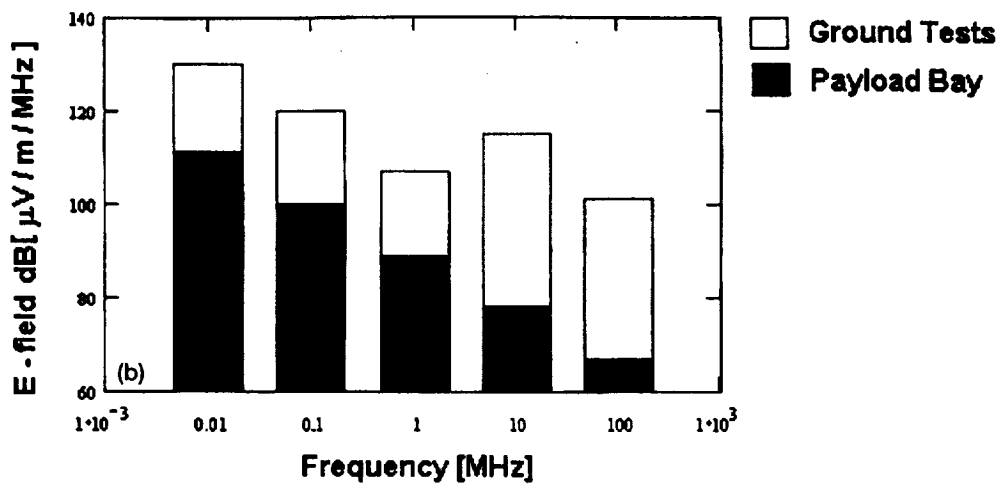
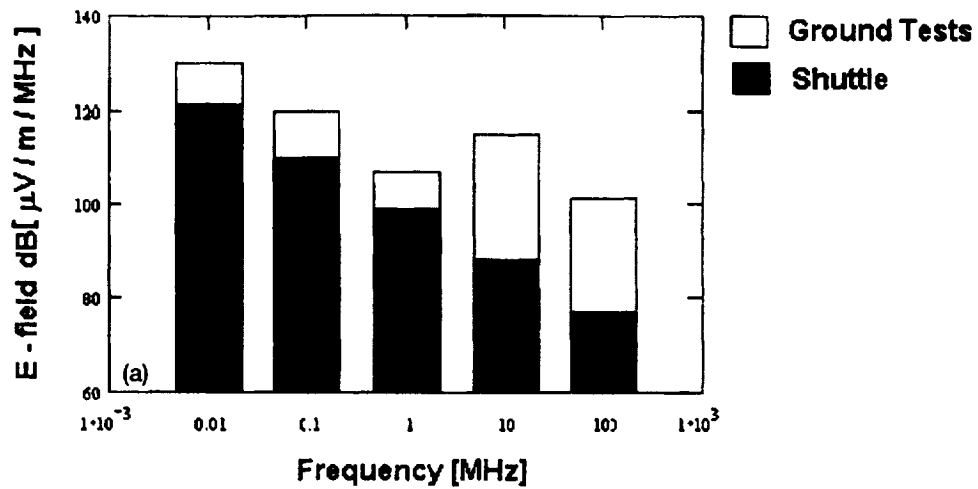


Figure 6.—(a) Comparison of max EMI levels set for Shuttle and EMI levels obtained from arcs at approximately 1 m distance in ground testing at LeRC. (See ref. 11 for details).
 (b) Comparison of max EMI levels set for payload in Shuttle payload bay and EMI levels obtained from arcs at \approx 1 m distance from plate at LeRC. (See ref. 11 for details).

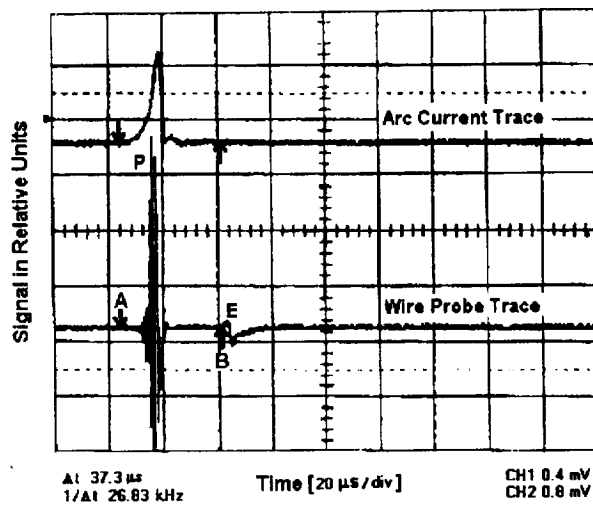


Figure 7.—Typical signal traces obtained from plasma cloud propagation tests. (Plate #1: $\phi_b = -400$ V, $C = 47 \mu\text{F}$, $R = 100 \text{ k}\Omega$).

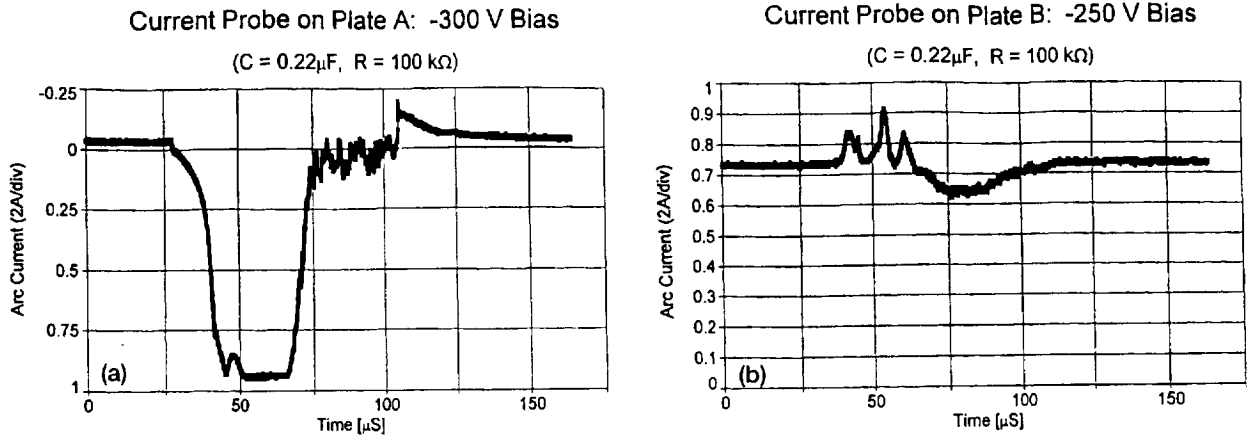


Figure 8.—Arc pulses recorded on two independently biased parallel plates. Note: distance between plates in 50 centimeters. (No measured delay was observed.)

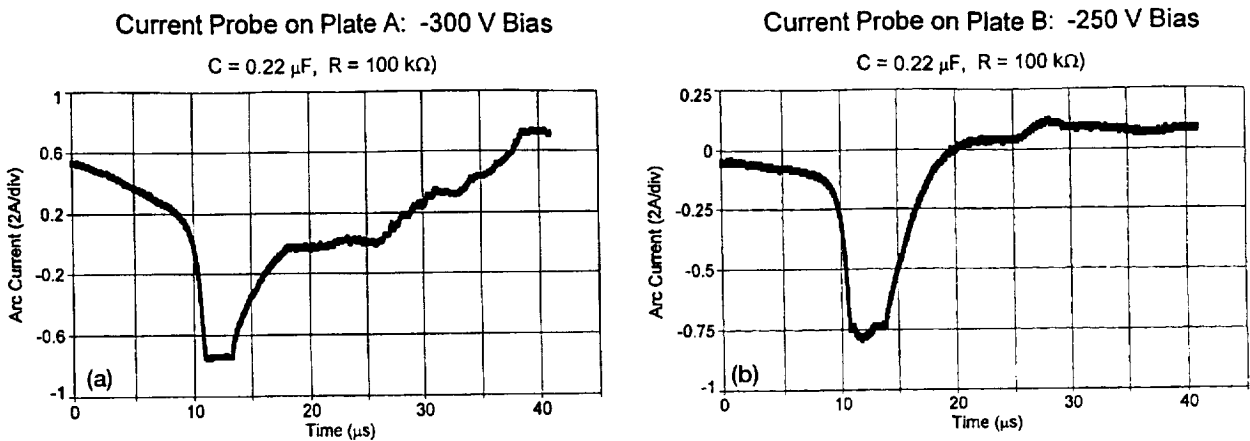


Figure 9.—Induced arcing between two independently biased parallel plates. Note: distance between plates in 25 centimeters. (No measured delay was observed.)

REPORT DOCUMENTATION PAGE			Form Approved OMB No. 0704-0188	
Public reporting burden for this collection of information is estimated to average 1 hour per response, including the time for reviewing instructions, searching existing data sources, gathering and maintaining the data needed, and completing and reviewing the collection of information. Send comments regarding this burden estimate or any other aspect of this collection of information, including suggestions for reducing this burden, to Washington Headquarters Services, Directorate for Information Operations and Reports, 1215 Jefferson Davis Highway, Suite 1204, Arlington, VA 22202-4302, and to the Office of Management and Budget, Paperwork Reduction Project (0704-0188), Washington, DC 20503.				
1. AGENCY USE ONLY (Leave blank)	2. REPORT DATE April 1999	3. REPORT TYPE AND DATES COVERED Technical Memorandum		
4. TITLE AND SUBTITLE Electrical Breakdown of Anodized Structures in a Low Earth Orbital Environment			5. FUNDING NUMBERS WU-632-1A-10-00	
6. AUTHOR(S) J.T. Galofaro, C.V. Doreswamy, B.V. Vayner, D.B. Snyder and D.C. Ferguson				
7. PERFORMING ORGANIZATION NAME(S) AND ADDRESS(ES) National Aeronautics and Space Administration John H. Glenn Research Center at Lewis Field Cleveland, Ohio 44135-3191			8. PERFORMING ORGANIZATION REPORT NUMBER E-11574	
9. SPONSORING/MONITORING AGENCY NAME(S) AND ADDRESS(ES) National Aeronautics and Space Administration Washington, DC 20546-0001			10. SPONSORING/MONITORING AGENCY REPORT NUMBER NASA TM-1999-209044	
11. SUPPLEMENTARY NOTES J.T. Galofaro, D.B. Snyder and D.C. Ferguson, NASA Glenn Research Center; C.V. Doreswamy, Tuskegee University, Tuskegee, Alabama 36088; B.V. Vayner, Ohio Aerospace Institute, Cleveland, Ohio 44142. Responsible person, J.T. Galofaro, organization code 5410, (216) 433-2294.				
12a. DISTRIBUTION/AVAILABILITY STATEMENT Unclassified - Unlimited Subject Category: 18 This publication is available from the NASA Center for AeroSpace Information, (301) 621-0390.			12b. DISTRIBUTION CODE Distribution: Nonstandard	
13. ABSTRACT (Maximum 200 words) A comprehensive set of investigations involving arcing on a negatively biased anodized aluminum plate immersed in a low density argon plasma at low pressures ($P_0 \approx 7.5 \times 10^{-5}$ Torr) have been performed. These arcing experiments were designed to simulate electrical breakdown of anodized coatings in a Low Earth Orbital (LEO) environment. When electrical breakdown of an anodized layer occurs, an arc strikes, and there is a sudden flux of electrons accelerated into the ambient plasma. This event is directly followed by ejection of a quasi-neutral plasma cloud consisting of ejected material blown out of the anodized layer. Statistical analysis of plasma cloud expansion velocities have yielded a mean propagation velocity, $v = (19.4 \pm 3.5)$ km/s. As the plasma cloud expands into the ambient plasma, energy in the form of electrical noise is generated. The radiated electromagnetic noise is detected by means of an insulated antenna immersed in the ambient plasma. The purpose of the investigations is (1) to observe and record the electromagnetic radiation spectrum resulting from the arcing process. (2) Make estimates of the travel time of the quasi-neutral plasma cloud based on fluctuations to several Langmuir probes mounted in the ambient plasma. (3) To study induced arcing between two anodized aluminum structures in close proximity.				
14. SUBJECT TERMS Arcing; Experimental testing; Anodized coatings; Plasmas; Electrical breakdown			15. NUMBER OF PAGES 17	
			16. PRICE CODE A03	
17. SECURITY CLASSIFICATION OF REPORT Unclassified	18. SECURITY CLASSIFICATION OF THIS PAGE Unclassified	19. SECURITY CLASSIFICATION OF ABSTRACT Unclassified	20. LIMITATION OF ABSTRACT	